Entanglement branching operator

Kenji Harada
Graduate School of Informatics, Kyoto University, Kyoto 606-8501, Japan

(Received 5 October 2017; revised manuscript received 19 December 2017; published 16 January 2018)

We introduce an entanglement branching operator to split a composite entanglement flow in a tensor network which is a promising theoretical tool for many-body systems. We can optimize an entanglement branching operator by solving a minimization problem based on squeezing operators. The entanglement branching is a new useful operation to manipulate a tensor network. For example, finding a particular entanglement structure by an entanglement branching operator, we can improve a higher-order tensor renormalization group method to catch a proper renormalization flow in a tensor network space. This new method yields a new type of tensor network states. The second example is a many-body decomposition of a tensor by using an entanglement branching operator. We can use it for a perfect disentangling among tensors. Applying a many-body decomposition recursively, we conceptually derive projected entangled pair states from quantum states that satisfy the area law of entanglement entropy.

DOI: 10.1103/PhysRevB.97.045124

I. INTRODUCTION

In the last decade, a tensor network grows a new promising theoretical tool for treating many-body systems. A novel property of a quantum state like a topological order [1] and a symmetry protected topological order [2] can be explicitly constructed by tensor networks. Tensor networks help us to understand novel properties of a quantum state as a specific property of a tensor. Based on the area law of entanglement entropy, we can define a general class of quantum states as a tensor network which has a special structure. For example, projected entangled pair states (PEPS) [3] and multiscale entanglement renormalization ansatz (MERA) [4]. We can control the quality of these tensor network states through the degrees of freedom on tensor indexes. Thus, we can use a tensor network as a promising variational wave function for strongly correlated materials. We can also define tensor network formulation of many-body problems. It gives us a new perspective way to treat many-body problems. For example, contracting a tensor network with controllable accuracy, we can systematically calculate the property of many-body systems.

To optimize a tensor in a tensor network and to calculate a contraction of a tensor network, novel numerical algorithms for a tensor network have been proposed in the last decades [5–10]. They help us to understand the properties of strongly correlated materials numerically (for example, see Refs. [11–14]). Thus, the development of tensor algorithms is highly active. However, the types of operations in a tensor network algorithm are limited.

In this paper we will propose a new tensor operation which is called an entanglement branching (EB). The EB is to split a composite entanglement flow in a link of a tensor network. We will explicitly introduce an EB operator in a tensor network.

In Sec. II we will briefly introduce tensor networks, tensor operations, and tensor network algorithms. In Sec. III we will define an EB operator and a local problem to optimize it. In Sec. IV we will show two applications of the EB operation. One is an improvement of the higher-order tensor renormalization group (HOTRG) [8] to catch a proper renormalization flow in a tensor network space. The other is a many-body decomposition of a tensor. In Sec. V we will conclude and discuss our results.

II. TENSOR NETWORKS, TENSOR OPERATIONS, AND TENSOR NETWORK ALGORITHMS

A tensor network is a theoretical tool to describe correlations between elements in a system. At first we will introduce a useful graphical notation for tensor networks. Second, we will introduce conventional operations in tensor networks. Finally, we will show an example of tensor network algorithms.

Figure 1 shows a graphical representation of a tensor and a tensor network. The object in Fig. 1(a) represents a tensor T. Each line from the object represents each index of T. The link (labeled m) between tensor L and R in Fig. 1(b) represents a tensor contraction for a tensor L index and a tensor R index. Thus, the whole of Fig. 1(b) represents a composite tensor (LR): $(LR)_{ijkl} \equiv \sum_m L_{ijm} R_{mkl}$. Figure 1(c) represents a complex composite tensor which consists of four tensors. Since these diagrams visually seem to be networks of tensors, they are called tensor networks.

A quantum state is defined in a tensor product space of localized Hilbert spaces. Thus, if we can regard a tensor index as the degrees of freedom in a localized Hilbert space, the wave function is written as a tensor. For example, we can regard four indexes i, j, k, and l in Figs. 1(a), 1(b) and 1(c) as the physical degrees of freedom in a four-body system. A quantum state defined by a tensor network is called a tensor network state. We can use a tensor network state to represent a novel quantum state explicitly [1,2]. If a tensor network state satisfies the area law of entanglement entropy as like PEPS and MERA, we can use it as a variational wave function which is systematically controllable. In general, an entanglement flows through a link of a tensor network. If we consider a cut of a tensor network to decompose physical indexes into two groups, the entanglement entropy of the decomposed subsystem is

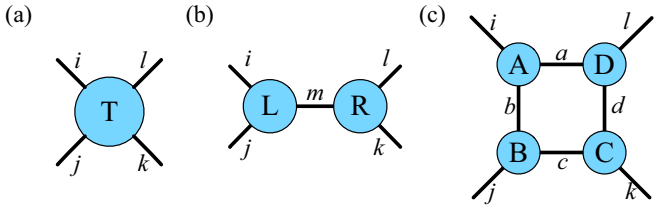

FIG. 1. (a) A graphical representation of a tensor T. Four lines represent tensor indexes i, j, k, and l. (b) A graphical representation of a tensor contraction between L and R. A link between two tensors denotes a pair of contracted indexes. For example, a link m represents a tensor contraction for the tensor L index and the tensor R index. Thus, this diagram represents a composite tensor (LR) as $(LR)_{ijkl} = \sum_m L_{ijm} R_{mkl}$. Applying a matrix decomposition, we can decompose a tensor into two tensors with a tensor contraction as shown in this diagram. (c) A tensor network which consists of four tensors, A, B, C, and D. We call it a four-body tensor network.

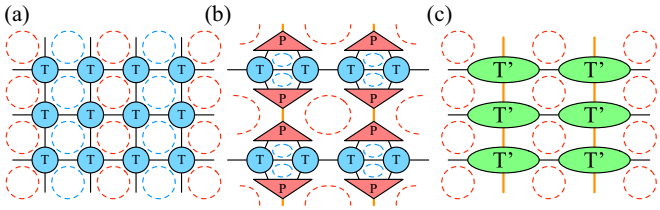

FIG. 2. (a) A tensor network representation of a partition function of a two-dimensional classical system or a one-dimensional quantum system. Dotted circles denote a short-range loop entanglement structure. Red and blue colors denote remained and erased entanglement flows by a HOTRG procedure, respectively. (b) A coarse-graining procedure in a HOTRG algorithm. A projection operator P is usually determined by a HOSVD. (c) A new renormalized tensor network for (a). A new tensor T' is the result of a tensor contraction of two Ts and two Ps in (b).

less than $\sum_{i\in\text{cut}} \log(D_i)$, where D_i is the degrees of a link i in a cut. Thus, a link i maximally contributes $\log(D_i)$ to an entanglement entropy. The minimum cut defines a limit of an entanglement entropy of a tensor network state. Therefore, the property of an entanglement entropy in a tensor network state depends on the geometrical structure of a tensor network.

There are two basic operations to manipulate a tensor network. One is a tensor contraction, and the other is a tensor decomposition. We calculate a tensor contraction in a tensor network to obtain a new composite tensor. For example, from Fig. 1(b) or 1(c) to 1(a). Currently, the tensor decomposition is simply based on a matrix decomposition. However, the matrix-based tensor decomposition has a limit of a transformation of tensor network topology. For example, using a matrix-based tensor decomposition, we can transform a tensor T in Fig. 1(a) to a tensor network of L and R in Fig. 1(b). However, we cannot transform Fig. 1(a) to 1(c). The matrix-based tensor decomposition produces only a two-body tensor network. Even the higher-order singular value decomposition (HOSVD) has the same limit that can be regarded as the sequence of two-body decomposition. The EB operation proposed in this paper will resolve this limit (see Sec. IV B).

Various types of tensor network algorithms have been proposed in the last decades [5–10]. Here we will give a brief introduction of the HOTRG algorithm [8] as a typical tensor network algorithm. A partition function of a classical or quantum system can be written by a grid-type tensor network as shown in Fig. 2(a). HOTRG algorithm approximately makes a coarse-grained tensor by inserting projection operators as shown in Fig. 2(b). We calculate projection operators from a HOSVD of a tensor T. Calculating tensor contractions among two Ts and two Ps, we obtain a coarse-grained tensor T' in Fig. 2(c). The number of tensors in the new tensor network is half. Thus, the HOTRG algorithm is a real-space renormalization on a tensor network. Repeating this procedure with changing a direction, we finally obtain a single tensor. A trace of a coarse-grained tensor is an approximation of all tensor contractions in the original tensor network. In general, as like the HOTRG algorithm, a procedure in a tensor network algorithm is a combination of tensor contractions and matrix-based tensor decompositions.

III. ENTANGLEMENT BRANCHING

A link in a tensor network carries an entanglement flow. The entanglement flow may be composite. For example, the entanglement flow in a link m of a tensor L in Fig. 1(b) may include two entanglement flows from i and j. Here we consider a splitting of a composite entanglement flow in a link as EB.

To define the EB operation explicitly, we introduce an isometric EB operator for a link of a tensor. For the sake of simplicity, we will discuss a splitting of a composite entanglement flow which consists of two entanglement flows. Figure 3(a) shows an EB operator B which splits a composite entanglement flow on a link m into upper left and right links (i and l). Here, based on a real space geometry, we consider that upper left and right links (i and l) of B should carry entanglement flows from lower left and right links j and k of T, respectively [see two dotted curves in Fig. 3(a)].

We can freely insert a pair of EB operators B and $B^\dagger$ on a link in a tensor network without approximation, because B is isometric [see Fig. 3(b)]. The insertion directly redesigns a tensor network to add new links which carry split entanglement flows. It gives us a new freedom to transform the topology of a tensor network as discussed in Sec. IV B.

To find an appropriate EB operator for a target link of a tensor T, we can use squeezing operators. Here we consider a new tensor network in Fig. 3(c). Tensors w and v in Fig. 3(c) are projection operators. If an entanglement flow from a lower left link j' of T passes to an upper left link i' of B in Fig. 3(c), we can construct a loop entanglement flow among T, B, and w [see a left dotted loop in Fig. 3(c)]. Thus we can squeeze the degrees

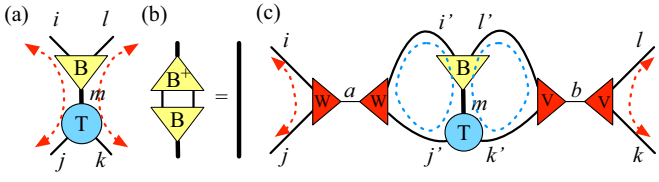

FIG. 3. (a) An EB operator B splits a composite entanglement flow on a link m into left and right directions. (b) An isometric property of an EB operator B. (c) A tensor network with squeezing operators w and v.

of freedom on a link a without increasing the distance between two tensor networks in Figs. 3(a) and 3(c). We can also squeeze that on a link b by the combination of T, B, and v. Therefore, if we can optimize a branching tensor B and projection operators w and v to squeeze the degrees of freedom of links a and b with minimizing the distance of tensor networks in Figs. 3(a) and 3(c), then the optimized tensor B is an appropriate EB operator. The minimization of the distance between tensor networks in Figs. 3(a) and 3(c) is a local optimization problem which depends only on T. To optimize tensors B, w, and v, we can use an iteration method in Appendix A.

We can extend the definition of an EB operator for a composite entanglement flow which consists of multiple entanglement flows than 2. The optimization problem can be generalized for such case straightforwardly.

IV. APPLICATIONS OF ENTANGLEMENT BRANCHING

The EB operation is a new freedom to manipulate a tensor network because it can split a composite entanglement flow on a link in a tensor network. In this section we will introduce two applications of the EB operation.

A. Improvement of HOTRG algorithm

We introduced the HOTRG algorithm in Sec. II as an example of tensor network algorithms. The HOTRG algorithm approximately calculates all tensor contractions in a grid-type tensor network [Fig. 2(a)]. We can apply it to calculate the partition function of classical and quantum many-body systems because a grid-type tensor network is a tensor network representation of a partition function.

While we can regard the HOTRG algorithm as a real-space renormalization group method on a tensor network as shown in Fig. 2, it may not be a proper real-space renormalization. In an ideal real-space renormalization, the effect of entanglements under a new cut-off scale should be renormalized. Thus, entanglement structures in a renormalized scale should be disappeared after a real-space renormalization. However, the HOTRG algorithm cannot erase a loop entanglement structure in a renormalized scale. Dotted loops in Fig. 2(a) mean loop entanglement structures in a tensor network. Here we assume that the entanglement of tensor T has a corner double-line (CDL) structure. Because loop entanglement structures are defined in a renormalized scale, they should disappear in a new renormalized tensor network of Fig. 2(c). While we can remove half of all loop entanglements by projection operators P in Fig. 2(b), half of them remain in a new renormalized tensor network as shown in Fig. 2(c). Therefore, a coarse-grained tensor by the HOTRG algorithm is not a proper renormalized tensor. There is the same problem in the tensor renormalization group (TRG) algorithm proposed by Levin and Nave [7] which is the first real-space renormalization group method for a grid-type tensor network. In fact, the invariant entanglement structure for these algorithms is CDL (see Ref. [15]). The idea to erase entanglements in a renormalized scale was first pointed by Gu and Wen [16]. However, their tensor-entanglement-filtering renormalization algorithm cannot correctly erase entanglements in a renormalized scale near a critical point. Evenbly and Vidal [9] proposed the use of disentangler tensors introduced in MERA to improve the TRG algorithm. Their tensor network renormalization (TNR) algorithm showed the expected property of an ideal real-space renormalization even at a critical point. Finally, the importance to erase entanglements in a renormalized scale was confirmed. In the following, we will consider the similar improvement of the HOTRG algorithm by the use of EB.

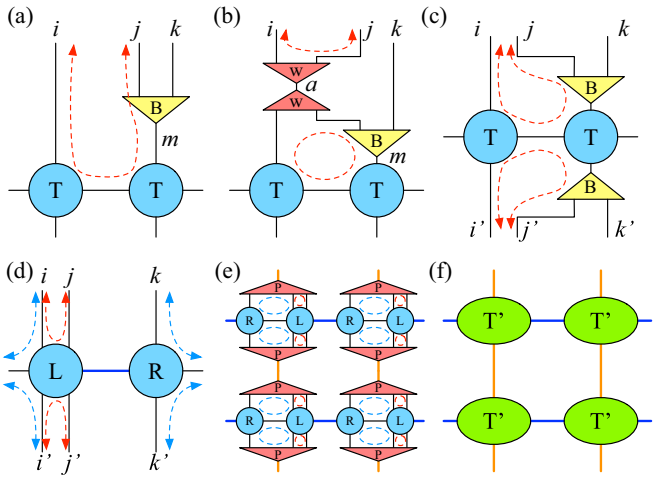

FIG. 4. The HOTRG algorithm with EB operations. Red and blue colors denote remained and erased entanglement flows by the original HOTRG procedure, respectively. (a) An EB operator B to separate a short-range entanglement flow. (b) A tensor network with squeezing operators w for the optimization of B. (c) Insertion of EB operators B in a grid-type tensor network. (d) New tensors L and R calculated by an SVD decomposition of a tensor network (c). (e) Insertion of projection operators P for a combination of R and L. (f) A new renormalized tensor network. A new tensor T' is the result of a tensor contraction of R and L and two Ps in (e).

The HOTRG procedure remains a part of loop entanglement flows which pass through four tensors around plaquettes [see dotted circles in Fig. 2(a)]. To catch the entanglement flow, we need to split a part of a composite entanglement flow on a link which belongs to a loop entanglement structure. Thus, we introduce an EB operator B on a link m as shown in Fig. 4(a). Since the contraction of B and $B^\dagger$ is identity, we can freely insert the pair into a link m. The purpose of inserting the EB operator is to catch an entanglement flow which constructs a loop entanglement structure through the nearest neighbor tensor [see the dotted curve in Fig. 4(a)]. To find an appropriate EB operator, the position of squeezing operators in an optimization problem is important. Here our purpose is to split the dotted entanglement flow in Fig. 4(a). If we insert squeezing operators on a left horizontal link from a tensor T connected to an EB operator B in Fig. 4(a), all entanglement flows from the left horizontal link to the link m are split into a link j. However, our target is an entanglement flow only in the shortest scale, not one in all scales. Figure 4(b) shows an effective position of squeezing operators to select only the target entanglement flow. The optimization problem of the EB operator B is a minimization of a distance between two tensor networks, Figs. 4(a) and 4(b). In general, an entanglement flow on a link is not perfectly composite. Even then, suitable squeezing operators in an optimization problem increase the ratio of a target entanglement component.

If we have an EB operator B to split an entanglement flow which constructs a loop entanglement structure, we can erase it by the conventional HOTRG procedure. We first gather the target entanglement flow in a tensor by SVD decomposing the tensor network in Fig. 4(c) into two tensors L and R in Fig. 4(d). For simplicity we assume a vertical flip symmetry of T. We set the bond dimension of a link between L and R as that of a horizontal link between two Ts. In general, the SVD decomposition may cause a truncation error. In the case of CDL tensors, the target entanglement flow is confined in the tensor L in Fig. 4(d). Between L and R, there is no entanglement flow which constructs the shortest loop entanglement structure. Thus, there is no truncation in the SVD decomposition into L and R. If we apply a coarse-graining procedure in the HOTRG algorithm to the combination of R and L as shown in Fig. 4(e), we can erase two loop entanglement structures by a single projection operator P. Finally, there is no loop entanglement structure in a new tensor network of Fig. 4(f). In summary, using an EB operator B, we define new tensors L and R from two tensors T. Applying the HOTRG algorithm to new tensor R and L, we can erase all loop entanglement structures in a renormalized scale. Therefore, this procedure may catch a proper renormalized flow in a tensor network space.

We test our HOTRG algorithm based on EB operators in the calculation of a partition function of the two-dimensional classical Ising model. Tensor network representation of the partition function of the two-dimensional Ising model is shown in Fig. 2(a). There are two directions in a grid-type tensor network in Fig. 2(a). To erase all loop entanglements in a renormalized scale, we apply the new HOTRG procedure shown in Fig. 4 to two tensor Ts linked horizontally. After that, we apply the conventional HOTRG procedure to two tensor T's linked vertically, because all loop entanglements are already removed. The definition of a renormalization step in the following is the pair of a new and a conventional HOTRG procedure for horizontally and vertically linked tensors. We initially prepare a tensor T for 2×2 sites of the two-dimensional Ising model. We set a limit of the bond dimension D of tensor T's indexes. The limits of bond dimensions of a link j and k of an EB operator B in Fig. 4(a) are $\sqrt{D}$ and D, respectively. To solve the optimization problem stably, we initially start the bond dimension of the link j from 1, and we gradually increase it to $\sqrt{D}$. For each bond dimension of the link j, we also gradually increase a bond dimension of a link a of a squeezing operator w in Fig. 4(b) from 1. The limit is an effective bond dimension (see the detail in Appendix A) of an original link of a tensor T. If a loop entanglement flow exists, the necessary bond dimension is less than the limit. In the increasing step of the bond dimension of the link j of B, we extend it as like a squeezing operator w in Appendix A. We notice that the order of a computational cost to solve the optimization problem does not change that of the total computational cost of a HOTRG algorithm. The former is $O(D^6)$, and the latter is $O(D^7)$ (see the details of the computational complexity of the new HOTRG algorithm in Appendix B).

Figure 5 shows the precision of free energy calculated by new and conventional HOTRG algorithms. Symbols joined by solid and dashed lines denote the relative precision of free energy by HOTRG algorithms with and without an EB operation, respectively. The precision of the new HOTRG

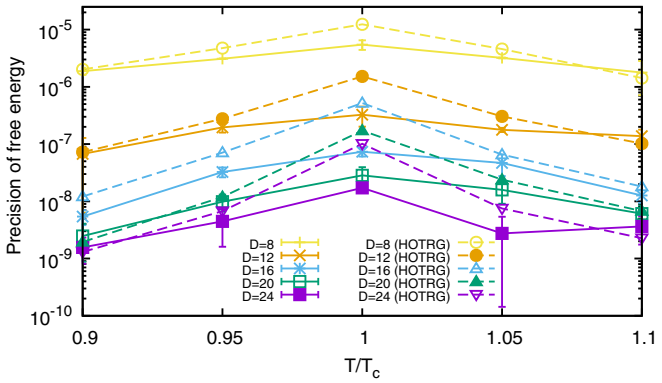

FIG. 5. Precision of free energy for the two-dimensional Ising model calculated by HOTRG algorithms with and without EB operation. A horizontal axis is a ratio of a temperature and a critical temperature T_c. D is the limit of a bond dimension of tensor index in Fig. 2(a). Results of HOTRG calculations with and without EB operation are joined by solid and dashed lines, respectively.

algorithm with the EB operation is better than that of the original HOTRG algorithm at all temperatures. In particular, the improvement is enhanced at the critical point [17]. The reason is that the original HOTRG algorithm cannot erase entanglements in a renormalized scale. To see the effect of an EB operator B, we check an entanglement between two tensors. In the following we define an entropy of a normalized singular value distribution of a tensor as $(-\mathrm{Tr}\tilde{\Lambda}\log\tilde{\Lambda})$, where $\tilde{\Lambda} = \Lambda/\mathrm{Tr}\Lambda$. Here Λ is a diagonal matrix of singular values for a matrix M which is a matrix representation of a tensor. Row and column indexes of M denote left and right parts of tensor indexes. The entropy of a composite tensor defined by a tensor network is an estimator of an entanglement flow through a link which connects two parts of a tensor network. Figure 6 shows the entropy of a composite tensor in the new HOTRG algorithm before and after applying EB operators at the critical point. Dashed lines in the inset of Fig. 6 are cuts to define a decomposition into left and right parts of a local tensor network before and after an EB operation. The entropy after EB operations is reduced from the original one. The

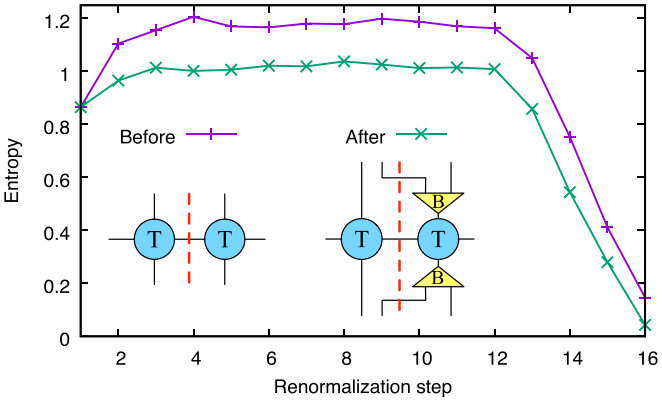

FIG. 6. Entropy of a composite tensor in a new HOTRG algorithm before and after EB operation at the critical point. The composite tensor is defined in the inset. A dotted line in the inset denotes a separation line between left and right parts of a composite tensor. Here the limit of a bond dimension is 24.

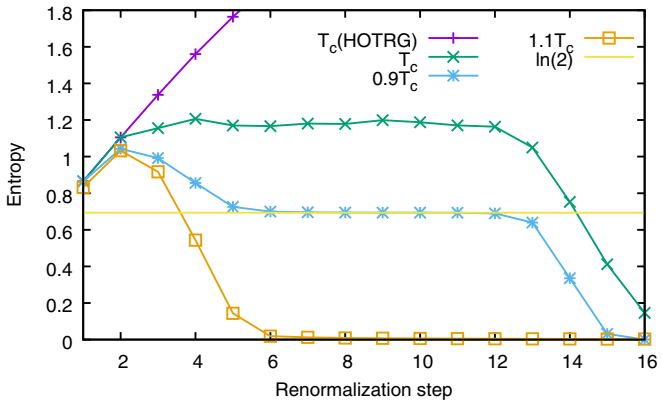

FIG. 7. Entropy of a composite tensor based on nearest neighbor tensors at three temperatures. T_c is a critical temperature. Here the limit of a bond dimension is 24 in all cases.

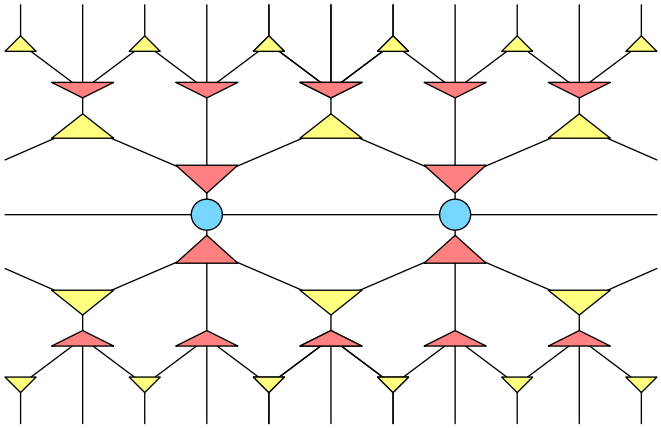

FIG. 8. A tensor network derived from a tensor network representation of a density operator by the HOTRG procedure with EB operation. A triangle with three links represents an EB operator. A triangle with four links represents a projection operator. A circle with four links represents a coarse-grained tensor.

entropy in Fig. 6 is reduced by applying EB operators. The EB operator splits a target entanglement flow correctly. Because of a decrease in an entanglement, we can regard this procedure as a disentangling operation. Figure 7 shows the entropy of a composite tensor based on nearest neighbor tensors (see the left tensor network in the inset of Fig. 6) at three temperatures. At the critical point, the entropy does not increase. However, that of the original HOTRG algorithm increases with the number of renormalization steps as like that of the TRG algorithm. The behavior of the new HOTRG algorithm is expected because we erase entanglements in a renormalized scale for each renormalization step. In disordered and ordered phases, the entropy converges to 0 and ln(2), respectively. These values are consistent with fixed point tensors in a disorder phase and an order phase. All behaviors are similar to that of TNR algorithm. From these results, we can confirm that the new HOTRG algorithm using an EB operator catches a proper renormalization flow in a tensor network space.

Evenbly and Vidal discussed the derivation of MERA from a density operator by using a TNR procedure [18]. The tensor network representation of a density operator of a one-dimensional quantum system is a grid-type tensor network shown in Fig. 2(a). Also, there are two open boundaries along the real-space direction. If we repeat a TNR procedure to the grid-type tensor network with two open boundaries, we finally obtain the product of two MERAs. Thus we can derive MERA from a tensor network representation of a density operator by TNR. If we repeat a new HOTRG procedure using an EB operator to a grid-type tensor network of a density operator, we obtain a tensor network shown in Fig. 8. Although a single link is split, the structure is similar to that of MERA. This new tensor network state also holds the log correction of the area law of entanglement entropy at a critical point of a quantum chain as like MERA.

B. Many-body decomposition

The conventional tensor decomposition is based on the matrix decomposition. It transforms a tensor to a two-body tensor network. For example, from (a) to (b) in Fig. 1. Thus, there is a limit of a transformation of tensor network topology.

If we use an EB operator, we can transform a tensor to a many-body tensor network as (c) in Fig. 1. Figure 9(a) shows a procedure of a many-body decomposition. At first, by using an SVD, a tensor T is decomposed into upper and lower tensors. It is a conventional two-body decomposition. If we insert a pair of EB operators on a contraction link between upper and lower tensors, we can split a composite entanglement flow in the link into left- and right-part entanglements. Contracting upper and lower tensors with EB operators, we get new upper and lower tensors with new left and right indexes. Decomposing new upper and lower tensors into subleft and subright tensors by using an SVD, we finally obtain a four-body tensor network. This procedure defines a four-body decomposition with a loop from a tensor T. It keeps a minimum entangled state on a loop because an isolated loop entanglement does not exist in an initial tensor. This procedure can be generalized for a many-body decomposition. We notice that this procedure is an approximate decomposition. We need to control the precision in the steps of SVD. Under a given precision, a necessary bond dimension of a new link depends on the strength of an entanglement flow.

The many-body decomposition may have interesting applications because it gives us a new freedom to transform a topology of a tensor network. The first application of a many-body decomposition is a perfect disentangling for a loop entanglement structure. The disentangling is an important idea

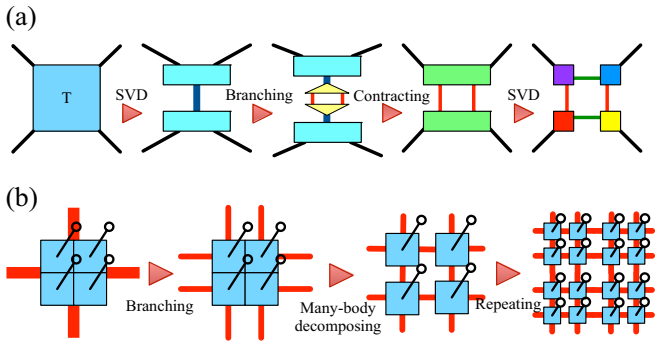

FIG. 9. (a) Many-body decomposition by EB operators. (b) Derivation of PEPS from a wave function.

for tensor network algorithms. For example, a disentangler tensor in MERA is a key role in expressing a critical quantum many-body state. The another example is a disentangler tensor in TNR. It is crucial to reach a proper fixed-point of critical phenomena by erasing a loop entanglement structure. One way of a perfect disentangling for a loop entanglement structure is a tensor contraction to erase a loop structure. We can perfectly remove a loop entanglement structure in a four-body tensor network of Fig. 1(c) by tensor contractions to Fig. 1(a). There is no loop entanglement in a tensor of Fig. 1(a). To inverse this deformation, by using a four-body decomposition shown in Fig. 9(a), we can again get a four-body tensor network without a loop entanglement structure. The second conceptual application of a many-body decomposition is a systematic derivation of PEPS from a wave function. Figure 9(b) shows a transformation of a tensor with four physical indexes which are represented by links terminated by open circles. We first apply EB operators to four unphysical indexes. EB operators split a composite entanglement flow from two nearest neighbor physical indexes. If we start from a wave function, we can skip this step, because there is no unphysical index. Because we recursively apply this step to a part of a derived PEPS in the following, we introduce this step. Second, we apply a variant of a four-body decomposition shown in Fig. 9(a). Finally, we get a PEPS which consists of 2×2 blocks. If a physical index is composite in a block, we recursively repeat this procedure. The many-body decomposition is approximate with precision. Under a fixed precision, a bond dimension of a derived PEPS depends on the strength of entanglements in a quantum state. If a quantum state satisfies the area law of entanglement entropy, we intuitively expect that this derivation succeeds by a finite bond dimension with accuracy. In fact, since the computational complexity is huge, this derivation of a PEPS is conceptual. However, this procedure shows that a metric of a tensor network state to describe a quantum state can be related to entanglements in a quantum state.

V. CONCLUSION AND DISCUSSION

A tensor network and a tensor network algorithm grow new promising theoretical tools to study various problems for many-body systems. To add a new freedom for a tensor network algorithm, we proposed an EB operation defined by an EB operator. It splits a composite entanglement flow on a tensor index. We can set up an optimization problem for splitting an entanglement flow by using a squeezing operator. The optimization problem can be solved iteratively.

We introduced two applications of an EB operation. The first one is an improvement of the HOTRG algorithm to catch a proper renormalization flow in a tensor network space. The numerical results for the two-dimensional Ising model show expected properties in a precision of a free energy calculation and a local entanglement between two coarse-grained tensors. We also derived a new tensor network state from applying our improved HOTRG procedure to a grid-type tensor network of a density operator. The second application is a many-body decomposition of a tensor. Using it, we can change a topology of a tensor network directly. We can apply it to a perfect disentangling and a systematic derivation of a PEPS from a wave function.

The purpose of an EB operation is to split a composite entanglement flow on a link in a tensor network. We can use it for a disentangling in a part of a tensor network as shown in the case of the improved HOTRG algorithm. Thus, the EB operator may be regarded as a disentangler in MERA and TNR. However, the purpose of a disentangler is different from that of an EB operator. It is a disentangling between two local degrees of freedom in a tensor network. In fact, a disentangler tensor does not consist only of a role of EB operation. For example, a disentangler tensor in TNR may contain both roles of projection and an EB. The disentangler is an important concept for tensor networks. The EB is a new basic operation which can be applied to the implementation of the disentangler. It may have other applications as a many-body decomposition.

From a practical point of view, the computational cost to optimize an EB operator is an issue. In particular, the number of iterations in the iteration method (see Appendix A) is a problem. In fact, in the case of the two-dimensional Ising model, we need more than 1000 iterations to solve the optimization problem of an EB operator. In the case of improved TRG algorithms, the computational cost of a loop optimization technique [10] and a Gilt technique [19] is much less than that of TNR [9,20]. Thus it extends the application scope of an improved TRG algorithm in a real study. For an optimization of an EB operator, we also need to reduce the total computational cost. Although we start from randomized initial tensors, there may be good initial tensors. To avoid a local solution, we extend tensor size gradually. There may be a good iteration strategy. The improvement of solving the optimization problem of an EB operator remains for future research.

Since the improved algorithms based on TRG as like TNR mix space and (imaginary-)time directions, they cannot be directly applied to anisotropic cases. However, the improved HOTRG algorithm with an EB operation can be applied to such problem, because it only does a coarse-graining of tensors along a chosen direction. Based on the same property, the HOTRG algorithm was extended to a three-dimensional grid-type tensor network [8]. The extension of our approach to a three-dimensional case is also interesting.

ACKNOWLEDGMENTS

The author appreciates conversations with N. Kawashima, S. Morita, and T. Suzuki, and, very specially, with T. Okubo, whose comment for the TNR algorithm was crucial to considering the optimization problem for an EB operator. This work was supported by JSPS KAKENHI Grants No. 26400392 and No. 17K05576, and by MEXT as Exploratory Challenge on Post-K computer (Frontiers of Basic Science: Challenging the Limits) and Priority Issue on Post-K computer (Creation of New Functional Devices and High-Performance Materials to Support Next-Generation Industries).

APPENDIX A: ITERATION METHOD TO OPTIMIZE AN ENTANGLEMENT BRANCHING OPERATOR

To optimize an EB operator in Fig. 3(a), we need to minimize a distance between two tensor networks of Figs. 3(a) and 3(c). An EB operator B and squeezing operators w and v are isometric. Thus, the minimization between two tensor networks of Figs. 3(a) and 3(c) is a maximization of a norm

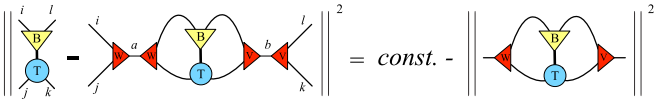

FIG. 10. A squared distance between two tensor networks to optimize an EB operator.

of a four-body tensor network by B, T, w, and v as shown in Fig. 10.

We can solve the maximization problem by iteration updates of B, w, and v. If we fix tensors except for a tensor w or v, the maximization problem for w or v can be written as a diagonalization problem. If we fix tensors except for a tensor B, we can solve the maximization problem for B by using an SVD optimization technique for MERA [21].

However, there may be many local solutions in the total maximization problem. To avoid a local solution, we use a strategy to extend a solution of w and v gradually. The procedure is written as follows:

(1) Initialize B randomly.

(2) Set the values of bond dimensions of links a and b 1, and initialize w and v randomly.

(3) Iteratively update B, w, and v to minimize the squared distance between Figs. 3(a) and 3(c). Because they are isometries, the local optimization problem for a tensor B can be solved by the singular value decomposition method as the optimization of isometries in MERA [21], and it for a tensor w or v can be solved by a diagonalization of an environment of a target tensor. Here we define an environment as a composite tensor of which a tensor contraction with target tensors is a maximized squared norm.

(4) Increase bond dimensions of links a and b (extend bond dimensions of w and v). New elements of w and v are initialized as zero, but other elements are unchanged. Alternatively, we can increase a bond dimension in a diagonalization of an environment of a target tensor w and v, respectively.

(5) Go back to step 3 until bond dimensions of links a and b reach a limit of them.

We can estimate the limit of bond dimensions of a link a and b by an entropy of a tensor T between an index of a target link and a composite index of other links.

Figure 11 shows entropy profiles in the above optimization process of EB operator in Fig. 10. The main panel shows a result of a CDL tensor with a random unitary on a target link of EB operator as follows:

$$T_{i_1 i_2, j_1 j_2, k_1 k_2} = U_{i_1 i_2, i_1' i_2'} \delta_{i_1', j_2} \delta_{i_2', k_2} \delta_{j_1, k_1}, \tag{A1}$$

where U is a random unitary and the composite index (i_1, i_2) is a target of EB operator. Thus, the ideal EB operator is $U^\dagger$. When the bond dimension of a subindex is $\sqrt{D}$, the entropy of a composite tensor of the ideal B and T is $\log(D)/2 (=\text{Entropy}_0)$ when it is decomposed into a left index group i and j and a right index group l and k. As shown in the main panel in Fig. 11, the entropy rapidly converges to the ideal value. A color of a symbol denotes a bond dimension of links a and b. Although we cannot expect an proper EB operator for a general random tensor T, the optimization method struggles to find a better EB operator. But, even for a random tensor, the optimization process decreases the entropy of a composite tensor as shown

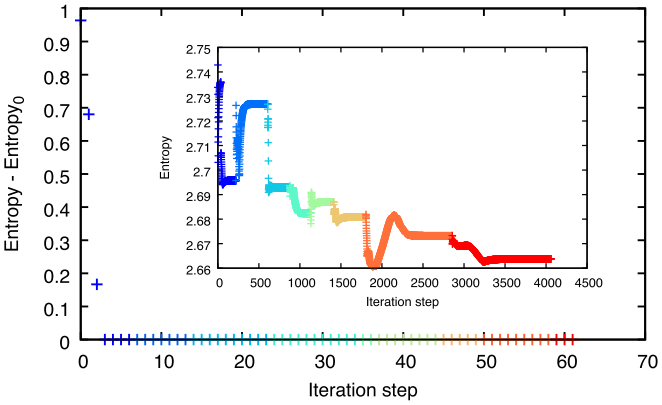

FIG. 11. Entropy profile of a composite tensor of B and T in an optimization process of EB operator in Fig. 10. The main panel shows a result of a CDL tensor with a random unitary on a target index. The bond dimension is $D = 3 \times 3$. Entropy$_0$ is log(3). The inset shows that of a random tensor for the same bond dimension. All tensors B, w, and v are randomly initialized. We start an initial bond dimension of links a and b from one. A color of a symbol denotes a bond dimension of links a and b.

in the inset of Fig. 11. Therefore, the proposed optimization method of EB operator is efficient.

APPENDIX B: COMPUTATIONAL COMPLEXITY OF A NEW HOTRG ALGORITHM WITH ENTANGLEMENT BRANCHING OPERATORS

The procedure of the new HOTRG algorithm with EB operators consists of three parts: (i) an optimization of an EB operator, (ii) a calculation of new tensor L and R, and (iii) a calculation of a coarse-grained tensor from L and R. For simplicity we suppose that the bond dimension of tensor indexes except for a link b in Fig. 12(a) is D and the bond dimension of the link b is $\sqrt{D}$.

The first part (i) is to solve a maximization of a squared norm of a tensor network by B, T, and w as shown in the right squared norm in Fig. 12(a). Since B and w are isometries, we can use an iteration method based on an SVD optimization technique as like MERA [21]. Thus, the computational complexity of the first part (i) is governed by the calculation of environments

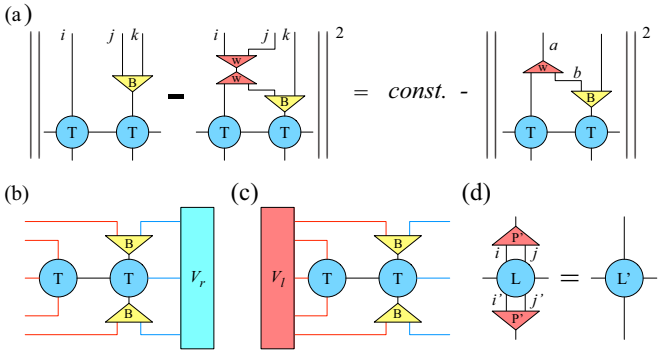

FIG. 12. The calculation in a new HOTRG algorithm with EB operators. (a) A squared distance between two tensor networks to optimize an EB operator. (b) A right matrix-vector multiplication. (c) A left matrix-vector multiplication. (d) A coarse-grained tensor L'.

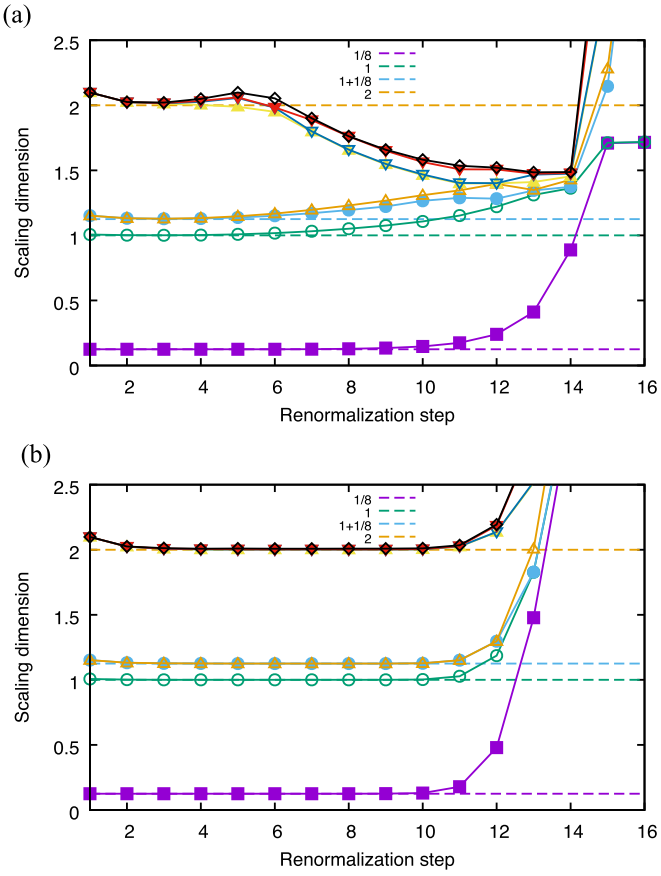

FIG. 13. Comparison of scaling dimensions for the original HOTRG and the new HOTRG algorithm with EB operators. (a) Scaling dimensions of the original HOTRG algorithm at a renormalization step. (b) Scaling dimensions of the new HOTRG algorithm with EB operators at a renormalization step. A transfer matrix is constructed from two columns of tensors (2×2 tensors). The bond dimension D is 24 in both cases. Dotted lines denote exact values of scaling dimensions of the two-dimensional Ising model.

for an SVD optimization technique. The environment is a composite tensor defined by a tensor network which is a representation of the squared norm in the right part of Fig. 12(a) except for a target tensor. The computational complexity of the calculation of an environment is $O(D^6)$. Also, the total computational time is proportional to the number of iterations to update tensors in the iteration method. As explained in Appendix A and Sec. IV A, we gradually increase the bond dimension of the link a and b in Fig. 12(a).

In the second part (ii) we use a partial SVD algorithm for the tensor network in Fig. 4(c) to decompose it into L and R in Fig. 4(d). We need to calculate a right and left matrix-vector multiplication for the partial SVD algorithm. They are shown in Figs. 12(b) and 12(c). Here V_r and V_l are right and left vectors, respectively. The computational complexity of their matrix-vector multiplications is $O(D^5)$. Thus, the total computational complexity of a partial SVD algorithm is $O(D^6)$.

In the third part (iii) we introduce an intermediate tensor L' which is applied to a projection operator for upward and downward indexes i, j, i', and j' of L. The bond dimension of upward and downward indexes of L' is D. The computational complexity of the calculation of L' is $O(D^6)$. Also, the computational complexity of the calculation of the coarse-grained tensor T' in Fig. 4(e) from L' and R is $O(D^7)$.

The maximum computational complexity is the third part (iii). Therefore, the total computational complexity of the new HOTRG algorithm with EB operators is $O(D^7)$.

APPENDIX C: CRITICAL FIXED-POINT TENSOR OF A NEW HOTRG ALGORITHM WITH ENTANGLEMENT BRANCHING OPERATORS

When we apply a new HOTRG procedure with EB operators to a renormalized tensor at a critical point, it quickly converges to a critical fixed-point tensor as shown in Fig. 7. There are several methods which derive a universal data from a critical fixed-point tensor. In particular, for a two-dimensional critical system, Gu and Wen [16] proposed a useful method based on a conformal field theory. Then, the scaling dimension can be estimated from eigenvalues of a transfer matrix constructed from a critical fixed-point tensor as follows:

$$\Delta_i = -\frac{1}{2\pi}\log(\lambda_i/\lambda_0), \tag{C1}$$

where λ_i is the ith eigenvalue of a transfer matrix defined by a renormalized tensor and λ_0 is the largest eigenvalue. Figure 13 shows scaling dimensions by Eq. (C1) at a renormalization step for the original HOTRG algorithm and the new one. We construct the transfer matrix from two columns of tensors ($L = 2$ transfer matrix in Ref. [10]). The bond dimension D is 24 in both cases. The high-level scaling dimensions of the original HOTRG algorithm start to merge with the low-level scaling dimensions after three renormalization steps. However, those of the new HOTRG algorithm with EB operators keep up to ten renormalization steps with 2^{22} spins. Therefore, EB operators improve a critical property of a renormalized tensor.

Table I shows the estimated values of scaling dimensions and a central charge of the new HOTRG algorithm with EB operators. The accuracy is comparable with the other entanglement-filtered tensor network algorithm (for example, see tables in Refs. [9,10,19,22]).

TABLE I. Exact values and numerical estimation of scaling dimensions and a central charge from a renormalized tensor by the new HOTRG algorithm with EB operators. A transfer matrix is constructed from two columns of tensors (2×2 tensors). The bond dimension D is 24. The last digit with parentheses means a confidential interval estimated from seven (2^{16} spins) to nine (2^{20} spins) renormalization steps.

	Exact	HOTRG with EB op.
c	0.5	0.49996(2)
σ	0.125	0.12515(3)
ϵ	1	1.0002(1)
	1.125	1.1250(1)
	1.125	1.1252(1)
	2	2.0009(2)
	2	2.0013(2)
	2	2.0029(4)
	2	2.008(1)

[1] N. Schuch, J. I. Cirac, and D. Perez-Garcia, PEPS as ground states: Degeneracy and topology, Ann. Phys. **325**, 2153 (2010).
[2] X. Chen, Z.-C. Gu, and X.-G. Wen, Classification of gapped symmetric phases in one-dimensional spin systems, Phys. Rev. B **83**, 035107 (2011).
[3] F. Verstraete, M. M. Wolf, D. Perez-Garcia, and J. I. Cirac, Criticality, the Area Law, and the Computational Power of Projected Entangled Pair States, Phys. Rev. Lett. **96**, 220601 (2006).
[4] G. Vidal, Entanglement Renormalization, Phys. Rev. Lett. **99**, 220405 (2007).
[5] T. Nishino and K. Okunishi, Corner transfer matrix renormalization group method, J. Phys. Soc. Jpn. **65**, 891 (1996).
[6] G. Vidal, Classical Simulation of Infinite-Size Quantum Lattice Systems in One Spatial Dimension, Phys. Rev. Lett. **98**, 070201 (2007).
[7] M. Levin and C. P. Nave, Tensor Renormalization Group Approach to Two-Dimensional Classical Lattice Models, Phys. Rev. Lett. **99**, 120601 (2007).
[8] Z. Y. Xie, J. Chen, M. P. Qin, J. W. Zhu, L. P. Yang, and T. Xiang, Coarse-graining renormalization by higher-order singular value decomposition, Phys. Rev. B **86**, 045139 (2012).
[9] G. Evenbly and G. Vidal, Tensor Network Renormalization, Phys. Rev. Lett. **115**, 180405 (2015).
[10] S. Yang, Z.-C. Gu, and X.-G. Wen, Loop Optimization for Tensor Network Renormalization, Phys. Rev. Lett. **118**, 110504 (2017).
[11] P. Corboz and F. Mila, Crystals of Bound States in the Magnetization Plateaus of the Shastry-Sutherland Model, Phys. Rev. Lett. **112**, 147203 (2014).
[12] P. Corboz, T. M. Rice, and M. Troyer, Competing States in the t-J Model: Uniform d-Wave State versus Stripe State, Phys. Rev. Lett. **113**, 046402 (2014).
[13] G. Evenbly and G. Vidal, Frustrated Antiferromagnets with Entanglement Renormalization: Ground State of the Spin-1/2 Heisenberg Model on a Kagome Lattice, Phys. Rev. Lett. **104**, 187203 (2010).
[14] K. Harada, Numerical study of incommensurability of the spiral state on spin-1/2 spatially anisotropic triangular antiferromagnets using entanglement renormalization, Phys. Rev. B **86**, 184421 (2012).
[15] H. Ueda, K. Okunishi, and T. Nishino, Doubling of entanglement spectrum in tensor renormalization group, Phys. Rev. B **89**, 075116 (2014).
[16] Z.-C. Gu and X.-G. Wen, Tensor-entanglement-filtering renormalization approach and symmetry-protected topological order, Phys. Rev. B **80**, 155131 (2009).
[17] At much far from a critical point, the precision of a new HOTRG algorithm with EB operators seems to be worse than that of the original HOTRG algorithm. At those points, there is not enough entanglement removed by an EB operator. Then, since the optimization problem is not well defined (see the inset in Fig. 11 of Appendix A), the obtained operator is not a proper EB. Therefore, an application of such an operator may obstruct the coarse-graining procedure in a HOTRG algorithm.
[18] G. Evenbly and G. Vidal, Tensor Network Renormalization Yields the Multiscale Entanglement Renormalization Ansatz, Phys. Rev. Lett. **115**, 200401 (2015).
[19] M. Hauru, C. Delcamp, and S. Mizera, Renormalization of tensor networks using graph-independent local truncations, Phys. Rev. B **97**, 045111 (2018).
[20] G. Evenbly, Algorithms for tensor network renormalization, Phys. Rev. B **95**, 045117 (2017).
[21] G. Evenbly and G. Vidal, Algorithms for entanglement renormalization, Phys. Rev. B **79**, 144108 (2009).
[22] M. Bal, M. Mariën, J. Haegeman, and F. Verstraete, Renormalization Group Flows of Hamiltonians Using Tensor Networks, Phys. Rev. Lett. **118**, 250602 (2017).